Rayleigh Number Criterion for Formation of A-Segregates in Steel Castings and Ingots

M. TORABI RAD, P. KOTAS, and C. BECKERMANN

A Rayleigh number-based criterion is developed for predicting the formation of A-segregates in steel castings and ingots. The criterion is calibrated using available experimental data for ingots involving 27 different steel compositions. The critical Rayleigh number above which A-segregates can be expected to form is found to be 17 ± 8. The primary source of uncertainty in this critical value is the dendrite arm spacing. The Rayleigh number criterion of the current study is implemented in a casting simulation code and used to predict A-segregates in three case studies involving steel sand castings. By comparing the predictions with observations made in the actual castings, the Rayleigh number criterion is shown to correctly predict the regions where no A-segregates form. However, the regions where A-segregates do form are somewhat over-predicted. Based on the results of the three case studies, the primary reason for this over-prediction is persumed to be the presence of a central zone of equiaxed grains in the casting sections. A-segregates do not form when the grain structure is equiaxed.

DOI: 10.1007/s11661-013-1761-4

I. INTRODUCTION

A-SEGREGATES are narrow, pencil-like macrosegregation patterns that are often found in the outer columnar zone of large steel ingots and castings. They contain small equiaxed grains and are highly enriched by various solute elements such as C, S, and P. Sometimes, A-segregates are associated with porosity and inclusions. A-segregates diminish the mechanical properties of a casting and should be avoided. For steel ingots, they can negatively affect subsequent rolling or forging operations. Shaped steel castings are sometimes rejected when A-segregates are exposed during machining. A-segregates are, in principle, the same as the freckles that are often observed in directionally solidified Ni-based superalloy castings.

A-segregates are initiated by convective instabilities during solidification in the high liquid fraction region of the semi-solid mush, near the primary columnar dendrite tips.[1] In solidification of steel, most of the light alloying elements (like C, S, and P) have a partition coefficient less than unity, implying less solubility in the solid than in the liquid. Therefore, during solidification, these elements will be rejected into the melt. The rejection of the light elements causes the density of the liquid to decrease. Under certain conditions, the density decrease is large enough that the induced buoyancy forces overcome the frictional retarding forces in the semi-solid mushy zone and convection cells form. Since the mass diffusivity of the liquid is much lower than its heat diffusivity, the segregated light liquid keeps its composition as it flows to the upper regions of the mushy zone where the temperature is higher. In these regions, the segregated melt causes delayed growth or even localized remelting of the solid, which leads to an increase in the local permeability of the mush. The local increase in the permeability allows the segregated liquid to flow more easily, which in turn delays solidification or enhances remelting further, until open channels form that are completely free of solid. The channels are no larger than a centimeter in diameter and are fed by melt flow from the surrounding mush. The channels emit highly segregated liquid into the central, still fully liquid, portion of a casting. The strong flow inside of the channels can separate solid fragments from the dendrites surrounding the channels. If the fragments remain in the channels, then they will eventually grow into the equiaxed grains that are associated with A-segregates. If the fragments are ejected into the central liquid region and survive, then they are a potent source of grains for the central equiaxed zone in castings.

The formation of A-segregates depends on a complicated interplay of numerous factors, including the thermal gradient, G; the speed of the isotherms, R; the structure and permeability of the semi-solid mush as dictated by the solid fraction and the dendrite arm spacings; and the variation of the liquid density in the mush as a function of the alloy composition and the segregation behavior of the various solute elements. Various criteria for the prediction and control of A-segregates or freckles can be found in the literature that are based solely on thermal parameters. Copley *et al.*[2] proposed a criterion for freckle formation that is based on a critical cooling rate, $\dot{T} = G \times R$. Their experiments showed that A-segregates will form if the cooling rate is

M. TORABI RAD, Graduate Research Assistant, and C. BECKERMANN, Professor, are with the Department of Mechanical and Industrial Engineering, The University of Iowa, 2402 SC, Iowa City, IA 52242. Contact e-mail: becker@engineering.uiowa.edu P. KOTAS, Postdoctoral Associate, is with the Department of Mechanical Engineering, Technical University of Denmark, Kgs, 2800 Lyngby, Denmark.

Manuscript submitted December 3, 2012.
Article published online May 8, 2013

below a critical value. Pollock and Murphy[3] suggested that, for Ni-based superalloys, freckles will form if the value of $G^{1/2}R^{1/4}$ is less than a critical value. For steel ingots, Suzuki and Miyamoto[4] suggested a criterion which is based on the value of $R^{2.1}G$. When $R^{2.1}G$ drops to less than a certain critical value, A-segregates are expected to form. This criterion is termed the Suzuki criterion in the current study. Yamada *et al.*[5] found that the critical value of $R^{2.1}G$ depends strongly on the composition of the steel. For the 27 different steel compositions that they investigated, the critical value of $R^{2.1}G$ varied by almost two orders of magnitude. Hence, the Suzuki criterion is not useful for predicting A-segregates unless the composition of the steel of interest corresponds exactly to one of the compositions for which the critical value was measured by Yamada *et al.*[5]

Since the formation of A-segregates and freckles is due to the competing effects of driving buoyancy forces and retarding frictional forces, the Rayleigh number is an appropriate dimensionless parameter to describe this convective instability.[6–11] If the Rayleigh number during solidification exceeds a certain critical value, then A-segregates or freckles can be expected to form. While the Rayleigh number does contain thermal parameters, a Rayleigh number criterion can be expected to be more generally valid than the above mentioned purely thermal criteria. The same value of the critical Rayleigh number can in principle be used for different compositions in the same alloy class (*e.g.*, for different steel compositions). This is because the Rayleigh number also contains the liquid density inversion and certain thermophysical properties. Furthermore, the Rayleigh number contains the permeability of the mush and, hence, accounts for the structure of the columnar dendrites. Nonetheless, it cannot be expected that the same value of the critical Rayleigh number is valid for any alloy and any casting system. This is because the Rayleigh number is not the only dimensionless parameter that governs convective instabilities during solidification.[11] A-segregate or freckle formation depends on numerous other characteristics of a solidification system, such as the geometry of the domain and the orientation of the thermal gradient or solidification front with respect to gravity.

Early examples where experimental results for freckle formation have been interpreted in terms of a Rayleigh number can be found in several studies.[12–14] Beckermann *et al.*[15] developed a Rayleigh number-based freckle predictor for directionally solidified Ni-based superalloy castings. Yang *et al.* 16 compared different versions of the Rayleigh number for freckle analysis. Ramirez and Beckermann[17] compared critical Rayleigh numbers for freckle formation in Pb-Sn alloys and Ni-based superalloys. Tewari and Tiwari[18] identified a mushy zone Rayleigh number that takes into account the role of dendrite side branching. Very recently, Yuan and Lee[19] applied a microstructural simulation model to predict the critical Rayleigh number for Pb-Sn alloys.

The objective of the current study is to develop a Rayleigh number criterion for predicting the formation of A-segregates in steel castings and ingots. A-segregates in steel have been predicted for almost 20 years using complex direct numerical simulations of the melt flow during solidification.[20] Such simulations are computationally very demanding. In fact, available computational resources are insufficient to numerically resolve pencil-sized A-segregates on the scale of typical commercial steel castings or ingots.[21,22] A simpler criterion for A-segregates, which requires only the knowledge of the steel composition and certain thermal parameters is still necessary. The Rayleigh number criterion of the current study for A-segregates in steel is developed using the experimental data of Suzuki and Miyamoto[4] and Yamada *et al.*[5] It is then implemented in a standard casting simulation code. Case studies are performed where the predictions from the Rayleigh number criterion are compared with observations of A-segregates in three different shaped steel sand castings.

II. CRITERIA FOR THE FORMATION OF A-SEGREGATES

A. *Suzuki Criterion*

The experimental studies conducted by Suzuki and Miyamoto[4] and Yamada *et al.*[5] show that the formation of A-segregates in steel ingots can be predicted by the following relationship[4,5]:

$$R^{1.1}\dot{T} = S \qquad [1]$$

where R is the solidification (or isotherm) speed in μm s^{-1}, $\dot{T}$ is the cooling rate in K s^{-1}, and S is termed here the Suzuki number in K s^{-1}(μm s^{-1})$^{1.1}$. The thermal parameters are evaluated at a temperature of 15 K less than the liquidus temperature, which for steel corresponds to a solid fraction of about 0.3. In the original studies,[4,5] the units used for R, $\dot{T}$, and S are mm min^{-1}, K min^{-1}, and K min^{-1}(mm min^{-1})$^{1.1}$, respectively; the unit conversion factor to convert S from K min^{-1}(mm min^{-1})$^{1.1}$ to K s^{-1}(μm s^{-1})$^{1.1}$ is 0.37. The solidification speed and the cooling rate are related to the temperature gradient by $G = \dot{T}/R$. As illustrated in Figure 1, A-segregates are initiated when the value of $R^{1.1}\dot{T}$ is less than a certain critical value of the Suzuki number. Conversely, no A-segregates are predicted to form when the value of $R^{1.1}\dot{T}$ is greater than the critical Suzuki number. Suzuki and Miyamoto[4] found that for 0.7 wt pct carbon steel (for the exact composition, see Case 1 in Table I), the value of the critical Suzuki number is S = 3.2 K s^{-1}(μm s^{-1})$^{1.1}$. Table I also includes the values of the critical Suzuki number for 26 other steel compositions. These values were extracted from Figures 3, 8, and 9 in Yamada *et al.*[5] The data in the table show that the critical Suzuki number depends strongly on the steel composition. These data are used in the current study to establish a Rayleigh number criterion for the prediction of A-segregates. Contrary to the Suzuki criterion, the Rayleigh number criterion is expected to result in a single critical value for all steel compositions.

B. *Rayleigh Number Criterion*

Various definitions of the Rayleigh number for predicting freckles and A-segregates in metal alloy

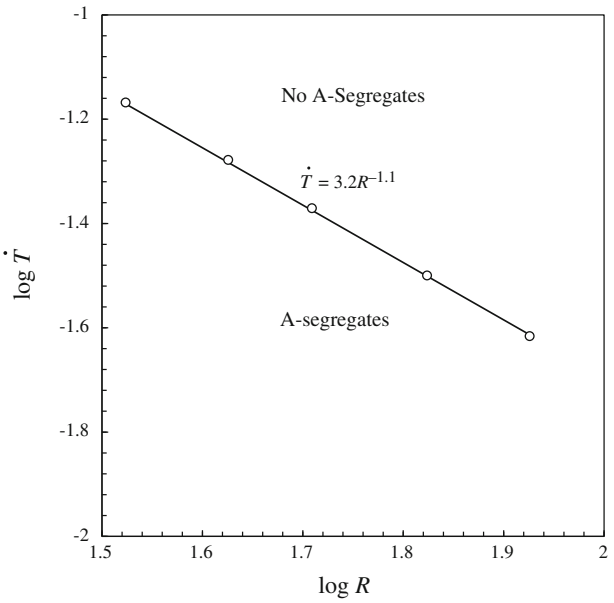

Fig. 1—Illustration of the Suzuki criterion for the formation of A-segregates in steel ingots.[4] The critical Suzuki value of $S = 3.2\ \mathrm{Ks^{-1}(\mu m\ s^{-1})^{1.1}}$ corresponds to Case 1 in Table I (0.7 wt pct carbon steel).

solidification have been reported in the literature.[16,17] The major difference between these definitions lies in a characteristic length scale (L) used in the definition. In the current study, following Ramirez and Beckermann,[17] $L = \alpha/R$ is used as the characteristic length scale, where α is the thermal diffusivity. Then, the Rayleigh number is given by Ramirez and Beckermann[17]

$$\mathrm{Ra} = \frac{\frac{\Delta\rho}{\rho_0} g \bar{K} L}{\alpha \upsilon} = \frac{\frac{\Delta\rho}{\rho_0} g \bar{K}}{R \upsilon} \qquad [2]$$

where υ is the kinematic viscosity of the liquid steel, g ($=9.81\ \mathrm{m\ s^{-2}}$) is the acceleration due to gravity, $\Delta\rho/\rho_0 = (\rho_0 - \rho)/\rho_0$ is the relative liquid density inversion over some initial portion of the mush, and $\bar{K}$ is the mean permeability of the initial portion of the mush. Freckles or A-segregates are predicted to form when the Rayleigh number exceeds a certain critical value. The dependence of the above Rayleigh number on thermal parameters is further explored below in Section II–C. The reason why the same critical Rayleigh number is obtained for different alloy compositions is that both the liquid density inversion and the mean permeability vary with alloy composition.

Table I. Critical Suzuki Values for Formation of A-Segregates in Steel Ingots Measured by Suzuki and Miyamoto[4] and Yamada *et al.*[5]

Case	Steel Type	Composition (wt pct) C	Si	Mn	P	S	Ni	Cr	Mo	V	Ti	S ($\mathrm{K\ s^{-1}(\mu m\ s^{-1})^{1.1}}$)
Small Experimental Ingot[4]												
1	carbon steel	0.69	0.47	0.62	0.017	0.014						3.2
Large Commercial Ingots[5]												
2	Cr-Mo	0.88	0.60	0.39	0.012	0.0008	0.19	2.86	0.21			1.9
3	Cr-Mo	0.89	1.00	0.33	0.018	0.010	0.16	2.90	0.38			3.4
4	carbon steel	0.30	0.32	0.66	0.009	0.017	0.13	0.10	0.06			0.36
5	Mn-Ni-Mo	0.19	0.30	1.35	0.007	0.008	0.76	0.06	0.49			0.21
6	Ni-Mo-V	0.31	0.35	0.55	0.018	0.019	3.12	0.09	0.42	0.07		0.44
7	Cr-Mo	0.29	0.25	0.7	0.010	0.012	0.29	1.16	0.35			0.24
8	Cr-Mo	0.28	0.06	0.67	0.010	0.007	0.20	1.06	0.35			0.09
9	carbon steel	0.33	0.31	0.76	0.008	0.007	0.28	0.24	0.10			0.48
10	Ni-Cr-Mo-V	0.25	0.05	0.26	0.007	0.012	3.66	1.69	0.44	0.12		0.07
11	Ni-Cr-Mo-V	0.26	0.05	0.26	0.005	0.010	3.98	1.79	0.45	0.12		0.05
12	Cr-Mo-V	0.27	0.24	0.75	0.003	0.002	0.18	1.17	1.22	0.28		0.14
13	Mn-Ni-Mo	0.22	0.26	1.41	0.007	0.007	0.76	0.11	0.52			0.21
Small Experimental Ingots[5]												
14	Mn-Ni-Mo	0.19	0.21	1.45	0.003	0.011	0.79	0.15	0.50			0.20
15	Mn-Ni-Mo	0.20	0.18	1.42	0.003	0.009	0.73	0.12	0.51			0.17
16	Mn-Ni-Mo	0.21	0.05	1.50	0.003	0.009	0.75	0.07	0.52			0.14
17	Mn-Ni-Mo	0.31	0.05	1.39	0.004	0.014	0.76	0.08	0.51			0.01
18	Mn-Ni-Mo	0.18	0.04	1.31	0.003	0.012	0.78	0.14	0.52			0.01
19	Ni-Cr-Mo-V	0.23	0.14	0.27	0.006	0.008	3.20	1.57	0.50	0.14		0.14
20	Ni-Cr-Mo-V	0.26	0.05	0.33	0.006	0.009	3.20	1.63	0.46	0.11		0.08
21	high carbon steel-standard	0.70	0.48	0.62	0.017	0.014	0.10	0.14	0.04			3.2
22	high carbon steel-Si	0.61	0.01	0.62	0.008	0.009	0.01	0.03	0.01			0.64
23	high carbon steel-Ni	0.67	0.50	0.60	0.010	0.012	1.01	0.10	0.05			1.2
24	high carbon steel-Cr	0.66	0.50	0.53	0.010	0.011	0.11	1.03	0.04			0.84
25	high carbon steel-Mo	0.70	0.56	0.64	0.010	0.013	0.11	0.08	1.09			0.24
26	high carbon steel-V	0.66	0.50	0.59	0.010	0.012	0.10	0.08	0.04	0.47		2.1
27	high carbon steel-Ti	0.63	0.59	0.63	0.009	0.011	0.11	0.09	0.04		0.65	1.2

In the current study, the Rayleigh number is evaluated over the first 30 pct of the mush. In other words, the liquid density inversion is evaluated as the difference between the density at the liquidus temperature, ρ_0 and the density, ρ, at a solid fraction of $g_s = 0.3$. The mean permeability, $\bar{K}$, is evaluated as the average solid fraction over the first 30 pct of the mush, *i.e.*, $\bar{g}_s \approx 0.5 \times g_s = 0.15$, which may be justified by the fact that in solidification of steel the initial portion of the solid fraction versus temperature relation is almost linear.[23] While the choice of evaluating the Rayleigh number over the first 30 pct of the mush (as opposed to, say, 20 pct) is relatively arbitrary, it reflects the fact that A-segregates initiate near the columnar dendrite tips. Using a different value for the solid fraction results in a different value of the Rayleigh number, but as long as a consistent evaluation method is used, a unique value of the critical Rayleigh number should result. Note that the choice of $g_s = 0.3$ is consistent with the method used by Suzuki and Miyamoto[4] and Yamada *et al.*[5] for evaluating the Suzuki number.

The mean permeability, $\bar{K}$, is obtained using the Blake–Kozeny equation[24]

$$\bar{K} = K_0 \frac{(1 - \bar{g}_s)^3}{\bar{g}_s^2} \qquad [3]$$

where K_0 is a reference permeability. Different methods have been used in the literature to evaluate the reference permeability as a function of the dendrite arm spacings. Schneider *et al.*[25] expressed the reference permeability as a function of the primary dendrite arm spacing, λ_1, as

$$K_0 = 6 \times 10^{-4} \lambda_1^2 \qquad [4]$$

Another common method is to calculate the reference permeability as a function of the secondary dendrite arm spacing, λ_2, from[24]

$$K_0 = \frac{\lambda_2^2}{180} \qquad [5]$$

It is emphasized that the two relations give the same reference permeability if $\lambda_1/\lambda_2 \approx 3$. This value for the ratio of the dendrite arm spacings is not unrealistic. In fact, Cicutti and Boeri[26] reported that in fully solidified continuously cast steel, $\lambda_1/\lambda_2 \approx 2$ to 3. Experimental and theoretical analyses of Imagumbai[27,28] show that $\lambda_1/\lambda_2 \approx 2$. For the prediction of A-segregates, it is preferable to use Eq. [4] involving the primary dendrite arm spacing, because during columnar dendritic solidification, the primary dendrite arm spacing is approximately constant, whereas the secondary dendrite arm spacing increases strongly with distance from the primary tips because of coarsening.[24] Moreover, for steel, no proven relations are available for this variation; all available secondary dendrite arm spacing relations are for the final spacing in the solidified steel, which has little relevance when trying to evaluate the permeability near the primary dendrite tips. Hence, Eq. [4] is used in the current study. The primary dendrite arm spacing is generally a function of the cooling rate, the alloy composition, and other variables. Specific relations for evaluating the dendrite arm spacing in steel solidification are provided in Section III–B.

Before proceeding, it is worthwhile discussing the use of the Blake–Kozeny equation for evaluating the mean permeability of the first 30 pct of the mush. It is well known that the Blake–Kozeny equation is likely to be inaccurate at low solid fractions.[29] However, using a permeability relation that has a different solid fraction dependency would simply result in a different value of the critical Rayleigh number. The only issue that is important to the current study is that the permeability is taken to be proportional to the square of the primary dendrite arm spacing. Given the general lack of knowledge of the morphology of the low solid fraction portion of the mush, taking $K \sim \lambda_1^2$ is believed to be the only viable choice. The use of the Blake–Kozeny equation should not be interpreted as implying that it is accurate for low solid fractions. Nonetheless, it allows the results of the current study to be compared with those of previous studies where the Blake–Kozeny equation was also used in the evaluation of the Rayleigh number.[15,17]

The thermophysical properties in the expression for the Rayleigh number are evaluated in the current study using the software JMatPro.[30] The values obtained for the liquid density inversion, $\Delta\rho$, are discussed in Section III–A. For all steel compositions in Table I, the kinematic viscosity and reference density are taken as $\upsilon = 8 \times 10^{-7} \text{m}^2\,\text{s}^{-1}$ and $\rho_0 = 7002\ \text{kg}\,\text{m}^{-3}$, respectively.

C. *Relation Between Suzuki and Rayleigh Number Criteria*

For a given composition, the Rayleigh number can be expressed solely as a function of the thermal parameters $\dot{T}$ and R. This can be accomplished by assuming that the dendrite arm spacing can be evaluated as a function of the cooling rate from a relation of the form $\lambda \sim \dot{T}^m$. Such a relation, with $m \approx -1/3$, is generally accepted for the final secondary dendrite arm spacing in a solidified casting,[24,31] but Taha *et al.*,[32] Jacobi and Schwerdtfeger[33] and Flemings *et al.*[34] have shown that for steels the same relation, with m close to 1/2 is valid also for the primary dendrite arm spacing. Substitution into Eq. [2] gives

$$\text{Ra} \sim \frac{\dot{T}^{2m}}{R} = R^{-1} \dot{T}^{2m}. \qquad [6]$$

Hence, for a given critical value of the Rayleigh number and a given composition, the Rayleigh number criterion can be written as

$$R^{(-1/2m)} \dot{T} = \text{constant} \qquad [7]$$

which is in the same form as the Suzuki criterion. In fact, the two criteria have the same dependence on the thermal parameters if $m = -1/(2 \times 1.1) = -0.45$. Given the above discussion of dendrite arm spacing relations, this value for m is realistic. In conclusion, the

Suzuki and Rayleigh number criteria have essentially the same dependence on the thermal parameters.

III. EVALUATION OF THE RAYLEIGH NUMBERS IN THE EXPERIMENTS OF SUZUKI AND MIYAMOTO[4] AND YAMADA *ET AL.*[5]

A. *Density Inversion*

The liquid density inversions obtained from JMatPro for the 27 steels in Table I are listed in Table II. Table II also provides the primary solid phase that forms in these steels up to $g_s = 0.3$. The liquid density inversion depends strongly on the solidification mode, because ferrite (δ) and austenite (γ) have different partition coefficients for the various elements present. As expected, the low-carbon steels in Table I generally have ferrite as the primary solid phase, whereas the high-carbon steels start to solidify as austenite. However, for the five low-carbon steels in Table I where the Ni content is greater than 3 wt pct (Cases 6, 10, 11, 19, and 20), the primary solid phase is predicted to be austenite.

The critical Suzuki numbers (last column in Table I) are plotted as a function of the liquid density inversion (third column in Table II) in Figure 2. The overall trend in this figure is that the critical Suzuki number increases with the increasing density inversion. Hence, the tendency for forming A-segregates generally increases with increasing density inversion. However, the critical Suzuki number is not a unique function of the density inversion. At a given density inversion, the critical Suzuki number can vary by as much as a factor of ten. This indicates that the formation of A-segregates is not only governed by the liquid density inversion, but also by other factors such as the permeability. Nonetheless, some interesting observations can be made. High-carbon steels (solid circles) have generally a higher $\Delta\rho$ than low-carbon steels, implying that they have a higher tendency for forming A-segregates. Increasing the contents of Si and Ti also increases $\Delta\rho$, whereas increasing the contents of Mo decreases $\Delta\rho$.

Table II. Primary Solid Phase, Liquid Density Inversion, and Calculated Rayleigh Numbers for the 27 Steels in Table I

Case	Primary Solid	$\Delta\rho$ (kg m^{-3})	Ra_O	Ra_{WT}
1	austenite	11.0	2.5	9.2
2	austenite	6.77	1.3	6.8
3	austenite	10.1	1.3	6.7
4	ferrite	8.14	11	23
5	ferrite	6.73	14	14
6	austenite	9.12	5.5	23
7	ferrite	6.13	8.8	22
8	ferrite	3.68	10	25
9	ferrite	5.67	6.2	15
10	austenite	3.07	4.5	23
11	austenite	2.37	3.8	22
12	ferrite	2.61	4.4	13
13	ferrite	6.08	13	16
14	ferrite	5.77	10	11
15	ferrite	4.53	9.3	11
16	ferrite	3.06	7.2	8.6
17	ferrite	4.38	12	28
18	ferrite	3.75	11	11
19	austenite	3.09	2.5	10
20	austenite	2.70	3.4	17
21	austenite	10.8	2.3	9.0
22	austenite	5.31	3.6	15
23	austenite	9.50	3.3	16
24	austenite	9.59	4.4	21
25	austenite	6.36	5.7	34
26	austenite	11.2	3.2	13
27	austenite	19.8	8.6	35

B. *Primary Dendrite Arm Spacing*

During the current study, numerous relations for the primary dendrite arm spacing in steel were examined.[31–37] Unfortunately, none of the available relations is valid for the entire range of steel compositions in Table I. It is not even clear from the literature, how the primary dendrite arm spacing depends on the primary solidification phase (ferrite or austenite). Therefore, a decision was made to calculate the final secondary dendrite arm spacing from correlations available in the literature, and then determine the primary dendrite arm spacing from the relation of Imagumbai:[27,28]

$$\lambda_1 = 2\lambda_2. \qquad [8]$$

Clearly, this procedure is only approximate, but in view of the discussion in Section II–B, it can be expected to provide reasonable estimates of the reference permeability. One should also keep in mind that the absolute value of the critical Rayleigh number is not significant; it is only important that a unique value for the critical Rayleigh number results for all 27 steels in Table I. Hence, the use of the factor 2 (instead of, say 3) in Eq. [8] should not distract.

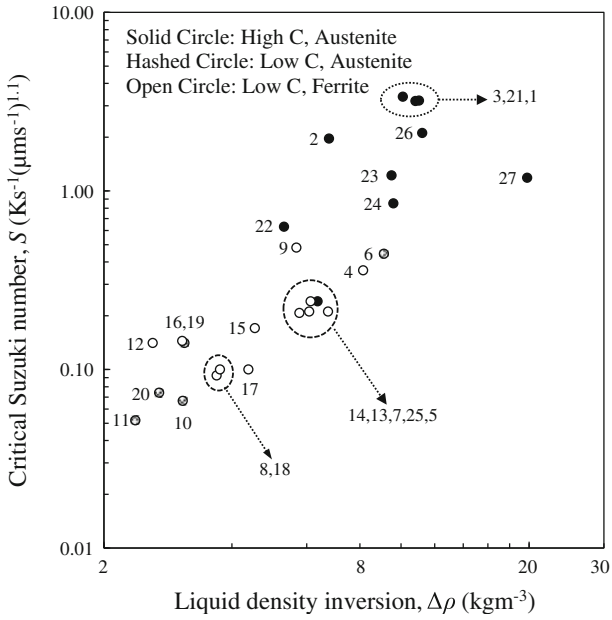

Fig. 2—Critical Suzuki number for the formation of A-segregates as a function of the liquid density inversion. The numbers correspond to the different cases in Table I.

In order to illustrate the importance of the choice of the dendrite arm spacing correlation, two different relations for steel are examined in the current study. The first one is by Ogino *et al*. (as published in Miettinen *et al*.[38])

$$\lambda_{2,O} = 123\dot{T}^{-0.33} e^{(-0.281C_C + 0.175C_{Mn} - 0.063C_{Cr} - 0.136C_{Mo} - 0.091C_{Ni})} \quad [9]$$

and the second one is by Won and Thomas[39]

$$\lambda_{2,WT} = \begin{cases} (1691 - 7209C_C) \times \dot{T}^{-0.4935} & \text{for } 0 < C_C < 0.15 \\ 143.9 \times \dot{T}^{-0.3616} C_C^{(05501 - 1996C_C)} & \text{for } C_C > 0.15 \end{cases} \quad [10]$$

where C_i is the concentration of solute i in wt pct, $\dot{T}$ is in K s^{-1}, and the resulting arm spacing is in μm. It should be noted that in these correlations, the exponent on the cooling rate varies from $m = -1/3$ to $m \approx -1/2$, which is in accordance with the discussion in Section II–C. Also note that all steels in Table I have a carbon content greater than 0.15.

The above relations for evaluating the dendrite arm spacings require the knowledge of the cooling rate. Unfortunately, the cooling rates could not be extracted from the original articles by Suzuki and Miyamoto[4] and Yamada *et al*.[5] To circumvent this problem, a procedure was adopted where the unknown cooling rate is replaced by the known critical Suzuki number for each alloy and an estimated solidification speed, R. Substituting the Suzuki number definition, Eq. [1], into Eq. [6] gives

$$\text{Ra} \sim \frac{\dot{T}^{2m}}{R} = \frac{S^{2m}}{R^{1+2.2m}} \quad [11]$$

With $m \approx -1/3$ from Eqs. [9] and [10] (for $C_C > 0.15$ wt pct), it can be seen that the exponent on R is only about 0.25. Hence, if an estimated R is consistently used, the resulting uncertainty in the Rayleigh number will be relatively small. For example, for a factor of 2 variation in R, the resulting variation in Ra will only be a factor of 1.19. This variation is still significant, but provides much better results than trying to estimate the cooling rate directly. Also note that for $m = -1/2$, which is still realistic, the exponent on R in Eq. [11] is equal to 0.1, which makes the Rayleigh number even less sensitive to R. Case 1 in Table I corresponds to a small 14 kg experimental ingot. Based on Figure 1, the solidification speed at which A-segregates form in this experimental ingot varies from $R = 32$ to 85 μm s^{-1}. Therefore, an approximate solidification speed of $R = 55$ μm s^{-1} is adopted for evaluating the Rayleigh number for all small experimental ingot cases in Table I (*i.e*., Case 1 and Cases 14 through 27). For the large commercial ingots of Cases 5, 7, and 8, figures in Yamada *et al*.[5] reveal that the solidification speed at which A-segregates form varies from $R = 18$ to 38 μm s^{-1}. Hence, a value of $R = 28$ μm s^{-1} is adopted for all large commercial ingot cases in Table I (Cases 2 through 13). As expected, the solidification speed in the large commercial ingots is generally less than the one in the experimental ingots. Finally, note that by means of the measured critical Suzuki number and an estimated solidification speed to determine the cooling rate, the primary dendrite arm spacing is evaluated using cooling conditions that prevail over the first 30 pct of the mush.

C. *Results for the Rayleigh Number*

Table II provides the calculated Rayleigh numbers for the Suzuki and Miyamoto[4] and Yamada *et al*.[5] experiments. The Rayleigh numbers evaluated using Eq. [9] are denoted by Ra_O and the ones using Eq. [10]

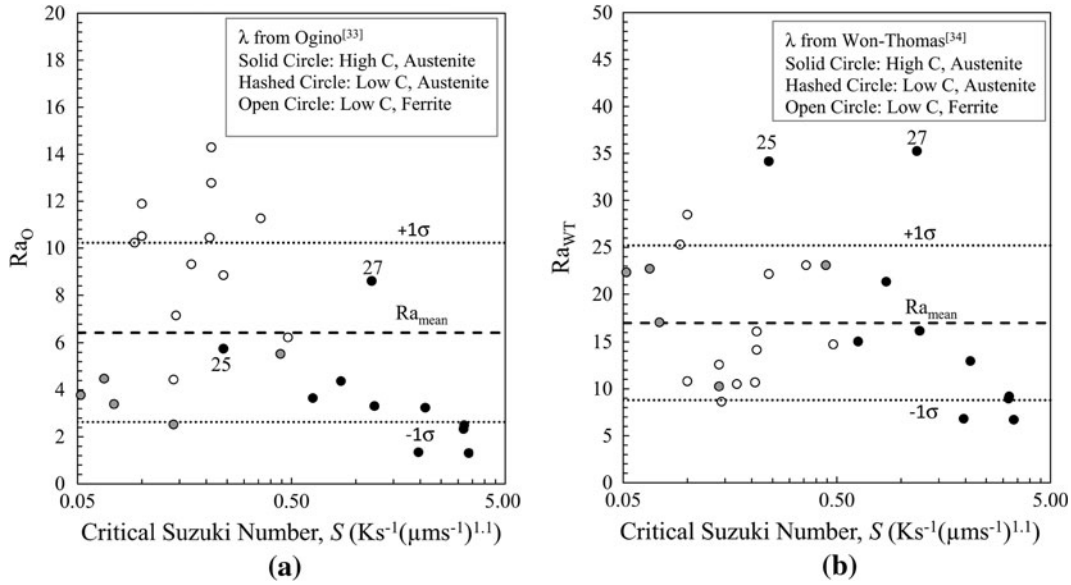

Fig. 3—Calculated critical Rayleigh numbers as a function of the Suzuki number: (*a*) dendrite arm spacings from Ogino *et al*. in Ref. [38]; and (*b*) dendrite arm spacings from Won and Thomas.[39]

are denoted by Ra_{WT}. These results are plotted in Figure 3 as a function of the critical Suzuki number. A log scale is used for the Suzuki number to show the entire two orders of magnitude range in the Suzuki number. The following observations can be made. Using the dendrite arm spacing relation from Ogino *et al.* in Reference 38 (Figure 3(a)), the Rayleigh numbers for the cases where ferrite is the primary solidification phase are consistently above those cases where austenite forms first. Case 27, which is the only steel with a significant Ti content, appears to be an outlier among the austenite cases. On the other hand, using the dendrite arm spacing relation from Won and Thomas[39] (Figure 3(b)) results in a much better overlap of the Rayleigh numbers for the cases where ferrite and austenite are the primary solidification phases. While this result is encouraging, there is still considerable scatter in the Rayleigh numbers. Now, Cases 25 and 27 appear to be outliers. The reason for the scatter and the outliers is not entirely clear, but could easily be attributed to uncertainties in the liquid density and dendrite arm spacing calculations. Note that the Won and Thomas[39] relation only accounts for the carbon content, but not for the concentrations of the other elements. In view of Eq. [9], it is clear that the dendrite arm spacing is a function of the contents of all alloying elements.

In lieu of better dendrite arm spacing relations, it is recommended to use the one by Won and Thomas,[39] since it better collapses the Rayleigh numbers to a single value. As can be seen from Figure 3(b), the mean value of the Rayleigh numbers for all 27 cases in Table I is equal to 17. Hence, the value of the critical Rayleigh number established in the current study for A-segregates in steel ingots is equal to 17. However, any value between 9 and 25 (plus/minus one standard deviation of the mean) could reasonably be taken as the critical Rayleigh number. This seemingly large spread in the critical value is well within the uncertainty in the current study of evaluating the Rayleigh number from the experiments. In most of the previous studies,[12–18] the Rayleigh numbers are plotted on a logarithmic scale. Such a scale would emphasize the fact that the critical Rayleigh numbers for the 27 cases in Table I vary by less than a factor of three, whereas the original Suzuki numbers vary by a factor close to 100. The effect of the uncertainty in the critical Rayleigh number on the prediction of A-segregates in steel castings is further discussed below in connection with the case studies.

If in Eq. (8) for the primary dendrite arm spacing a factor of three were used instead of two, then the critical Rayleigh number would be equal to 38. It is noteworthy that, using similar procedures as in the current study, Ramirez and Beckermann[17] found critical Rayleigh numbers of 38 to 46 for Pb-Sn alloys and 30 to 33 for Ni-based superalloys. Certainly, the critical value of the current study for steel is in reasonable agreement with the ones found previously for Pb-Sn alloys and Ni-based superalloys. However, this agreement may be fortuitous because the previous critical Rayleigh numbers are for freckles in upward directional solidification, whereas the one in the current case is for inclined A-segregates in ingot solidification.

IV. APPLICATION OF THE RAYLEIGH CRITERION TO PREDICT A-SEGREGATES IN STEEL CASTINGS

In this section, three case studies are presented where the Rayleigh number criterion is applied to predict A-segregates in shaped steel sand castings. The castings are simulated using the software package MAGMASOFT®.[40] Performing a casting simulation requires numerous process parameters and material properties to be specified. The current case study castings are adopted from previous investigations,[41–43] and the reader is referred to these studies for the details of the simulations. As a first approximation, filling of the mold and melt convection during solidification were not simulated. It was verified through additional simulations that for the relatively thick-walled castings examined in the current case studies, temperature non-uniformities at the end of filling do not have a significant effect on the predicted Rayleigh numbers. Not simulating melt convection during solidification can also affect the predicted temperatures. In order to approximate the thermal mixing of the melt by convection, the thermal conductivity of the liquid steel at temperatures greater than the liquidus temperature was enhanced by a factor of 2.5. However, additional simulations showed that this enhancement had a negligible effect on the predicted Rayleigh numbers. Using the melt convection simulation feature in MAGMASOFT® is not recommended because it does not predict A-segregates. Simulations of melt convection during solidification are highly inaccurate if the formation of A-segregates is not predicted or not fully resolved.[20–22] This is because much of the convection is due to highly segregated liquid flowing out of the open channels in the mush into the central, though fully liquid, portion of a casting.

The simulations provide the values of the thermal parameters necessary in the evaluation of the Rayleigh number. The thermal parameters are evaluated locally, at each position in the casting, such that a map of Rayleigh numbers over the entire casting is obtained. Details of the implementation of the Rayleigh number criterion within the casting simulation software are provided in the next section.

A. *Implementation of the Rayleigh Number Criterion in the Casting Simulation Software*

The Rayleigh number criterion of the current study, using the dendrite arm spacing relation by Won and Thomas[39] was implemented as a user result in the casting simulation software. This requires the Rayleigh number to be expressed in terms of the cooling rate and the temperature gradient, rather than in terms of the solidification speed. Substituting Eqs. [8] and [10] into Eq. [4] gives

$$K_0 = 49.70 \times 10^{-12} \dot{T}^{-0.7232} C_C^{1.1-3.99C_C}. \qquad [12]$$

Substituting this result into Eq. [3], and using $\bar{g}_s = 0.15$ (see Section II–B) gives

$$\bar{K} = 1.36 \times 10^{-9} \dot{T}^{-0.7232} C_C^{1.1-3.99C_C}. \qquad [13]$$

Substituting Eq. [13] into the Rayleigh number definition, Eq. [2], and using $\dot{T} = R \times G$ yields

$$\mathrm{Ra_{WT}} = 2.38 \times 10^{-6} \times C_C^{(1.1-3.99C_c)} \Delta\rho \frac{G}{\dot{T}^{1.7232}} \qquad [14]$$

where C_C is in wt pct, $\Delta\rho$ is in kg m^{-3}, G is in K m^{-1}, and $\dot{T}$ is in K s^{-1}. The thermal parameters, G and $\dot{T}$, are evaluated locally at the average temperature between the liquidus temperature and the temperature corresponding to $g_s = 0.3$. The compositions of the steels used in the three case studies are listed in Table III. The carbon content is directly substituted into Eq. [14]. Table III also provides the liquid density inversion that was obtained from JMatPro for each of the three compositions. The liquid density inversion is also substituted into Eq. [14].

B. *Case Study 1-Cubes*

The first case study considers four cube castings with different riser toppings and riser neck geometries.[36] Schematics of the castings are shown in Figure 4. All four castings are 0.254 m (10 in.) cubes, with 0.2 m (8 in.) diameter by 0.24 m (9.4 in.) high cylindrical risers at the top. The risers are surrounded by an exothermic sleeve. In the first casting, the riser is covered with dry sand after filling. The other three castings have an exothermic hot topping. In the first and second castings, the riser is placed directly on the top of the cube. In the third and fourth castings, a 2.54 cm (1 in.) thick breaker core is inserted between the cube and the riser. The inner diameter of the breaker core is 0.15 m (6 in., 75 pct open) for the third casting and 0.1 m (4 in., 50 pct open) for the fourth casting. Details of the simulations of these castings can be found in Carlson and Beckermann.[42]

Comparisons between the A-segregates observed in the four cube castings and the predicted Rayleigh numbers are presented in Figures 5 through 8. The figures show a vertical mid-thickness section through the castings. On the sections of the experimental castings (Figures 5(a) through 8(a)), A-segregates can be observed to form near the vertical side walls of the cubes, at approximately mid-height (red arrows). These A-segregates extend toward the cube–riser junction. As is typical for A-segregates, they are inclined relative to gravity. Additional A-segregates originate inside of the risers. The predicted Rayleigh numbers are plotted in Figures 5(b) through 8(b) on a scale from 17 to 25, with 17 being the mean and 25 being one standard deviation above the critical Rayleigh number as determined in Section III (see Figure 3(b)). It can be seen that the experimentally observed A-segregates all fall into regions where the Rayleigh number is predicted to be greater than the critical value of 17. Conversely, no A-segregates exist in the regions of the cubes where the

Table III. Composition and Liquid Density Inversion for the Steels in the Three Case Studies

	Composition (wt pct)											
Case Study	C	Si	Mn	P	S	Ni	Cr	Mo	Ti	Al	N	$\Delta\rho$ (kg m^{-3})
Cubes	0.36		0.76	0.028	0.02					0.048		7.7
Forging Ram	0.18	0.34	1.33	0.008	0.005	0.75	0.16	0.06	0.023	0.036	0.0069	6.95
Ring	0.3	0.4	1.35	0.0035	0.0035							7.97

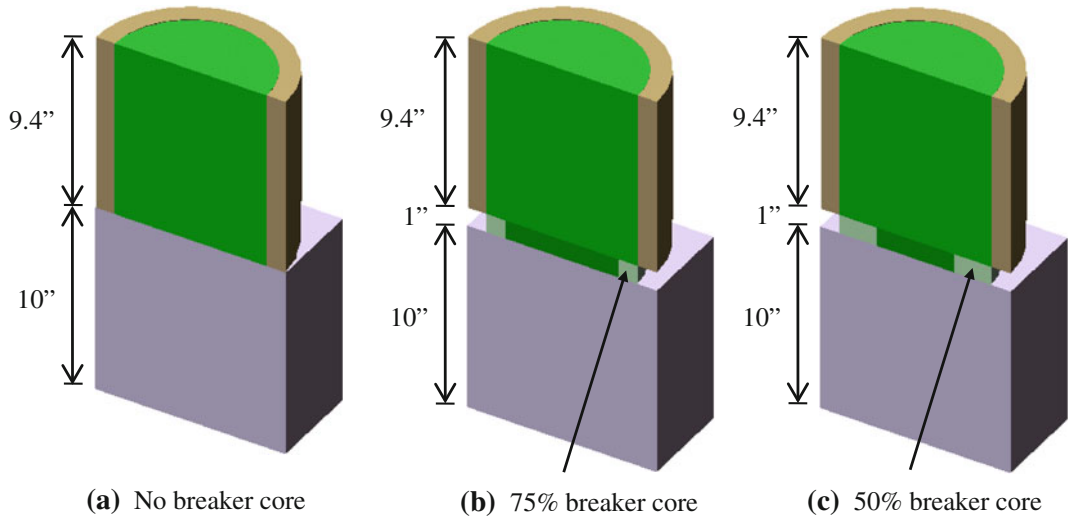

Fig. 4—Schematics of the cube castings of case study 1 (light purple: cube casting; green: riser; light green: breaker core; light brown: riser sleeve). All dimensions are in inches.

Rayleigh number is predicted to be less than the critical value. This comparison instills some confidence in the Rayleigh number criterion of the current study.

The Rayleigh number criterion is only intended to predict the onset of A-segregates, not their subsequent (non-linear) evolution. In other words, the Rayleigh number contours cannot be expected to provide the exact number and shape of the A-segregates. They only provide the regions where the conditions are favorable for the formation of A-segregates. The onset of the A-segregates near the vertical side walls of the cubes is further investigated in Figures 5(c) through 8(c). In these figures, the predicted Rayleigh numbers are plotted along a horizontal line that corresponds approximately to the height in the cubes where the A-segregates initiate. The measured distance of the onset of the A-segregates from the side walls is indicated by a vertical dashed line. It can be seen that for all four cubes, the onset of the A-segregates corresponds well to a critical Rayleigh number of 17 ± 8. The predicted Rayleigh numbers show a rather steep variation near the sidewalls. As a result, the uncertainty range for the current study in the critical Rayleigh number (9 to 25) corresponds to less than 2 cm in distance. Since the diameter of the A-segregates is about 1 cm, their appearance on a section of a casting depends strongly

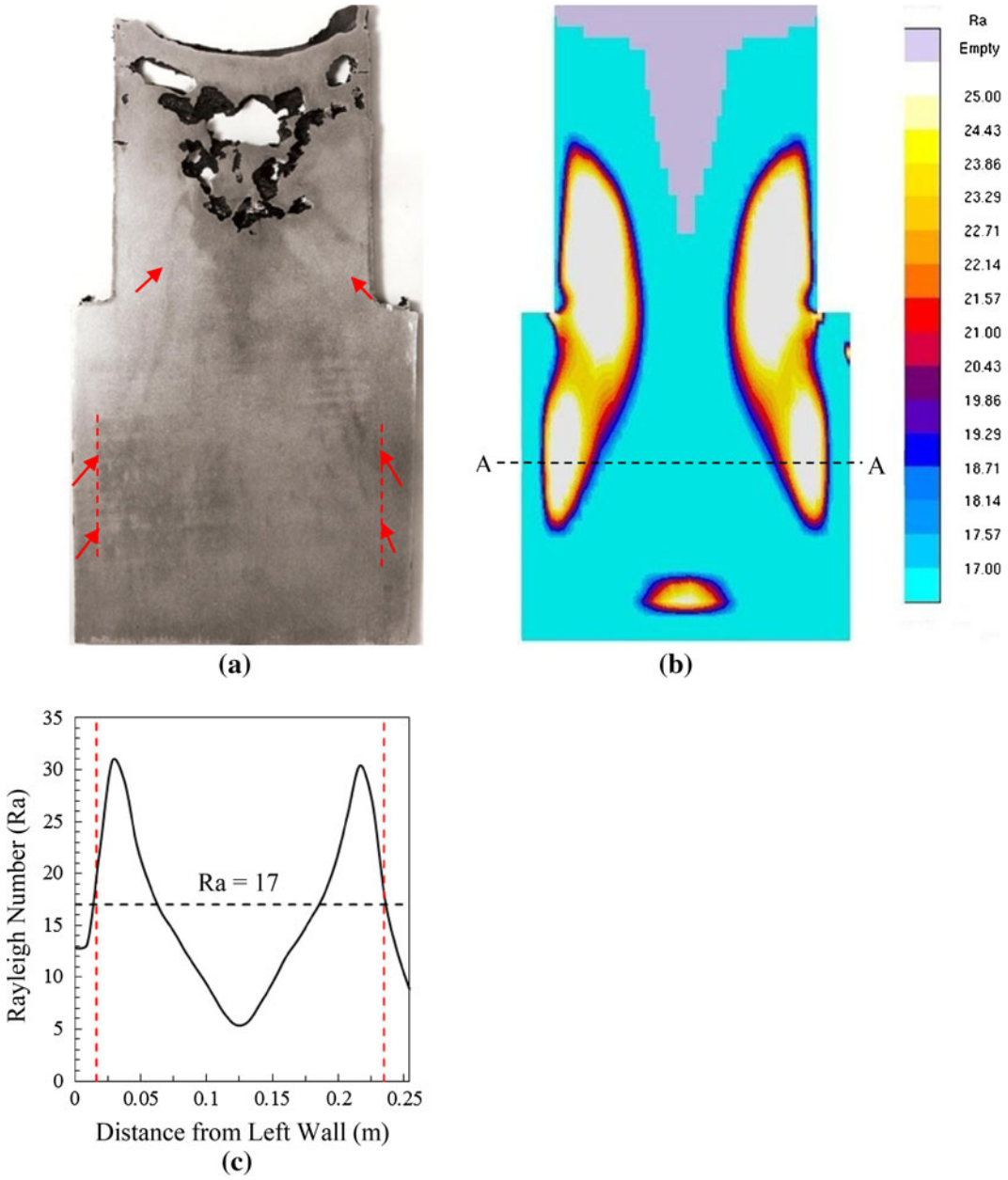

Fig. 5—Comparison of A-segregates (red arrows) observed in the cube casting with no breaker core and a dry sand topping: (*a*) with the predicted Rayleigh numbers, (*b*) for a vertical mid-thickness section. The predicted Rayleigh numbers along the dashed line A-A in (b) are plotted in (*c*). The vertical dashed lines in (a) and (c) indicate the onset of the A-segregates near the side walls. Photograph courtesy of Murphy.[41]

on where the cut is made. One cannot expect that the onset of A-segregates can be located on a single casting section with accuracy greater than ±1 cm. Therefore, the present spread in the critical Rayleigh number corresponds approximately to the uncertainty in locating the onset of the A-segregates in the castings.

Overall, the differences in the formation of A-segregates between the four cube castings are relatively minor. Nonetheless, with decreasing size of the opening that is formed by the breaker core between the cube and the riser, the tendency for A-segregates to form inside of the cubes appears to decrease. In particular for the 50 pct breaker core (Figure 8), the A-segregates near the vertical side walls of the cube are much shorter and less pronounced than in the two castings without a breaker core (Figures 5 and 6). This tendency is also predicted by the Rayleigh number criterion of the current study. Small isolated regions with supercritical values of the Rayleigh number are predicted directly adjacent to the breaker core of the fourth cube casting (Figure 8(b)), and A-segregates can indeed be observed to form in these regions (Figure 8(a)).

There are a few regions in the cube castings where the Rayleigh number is predicted to be greater than the critical value, but no A-segregates are observed experimentally. An example is given by the relatively small

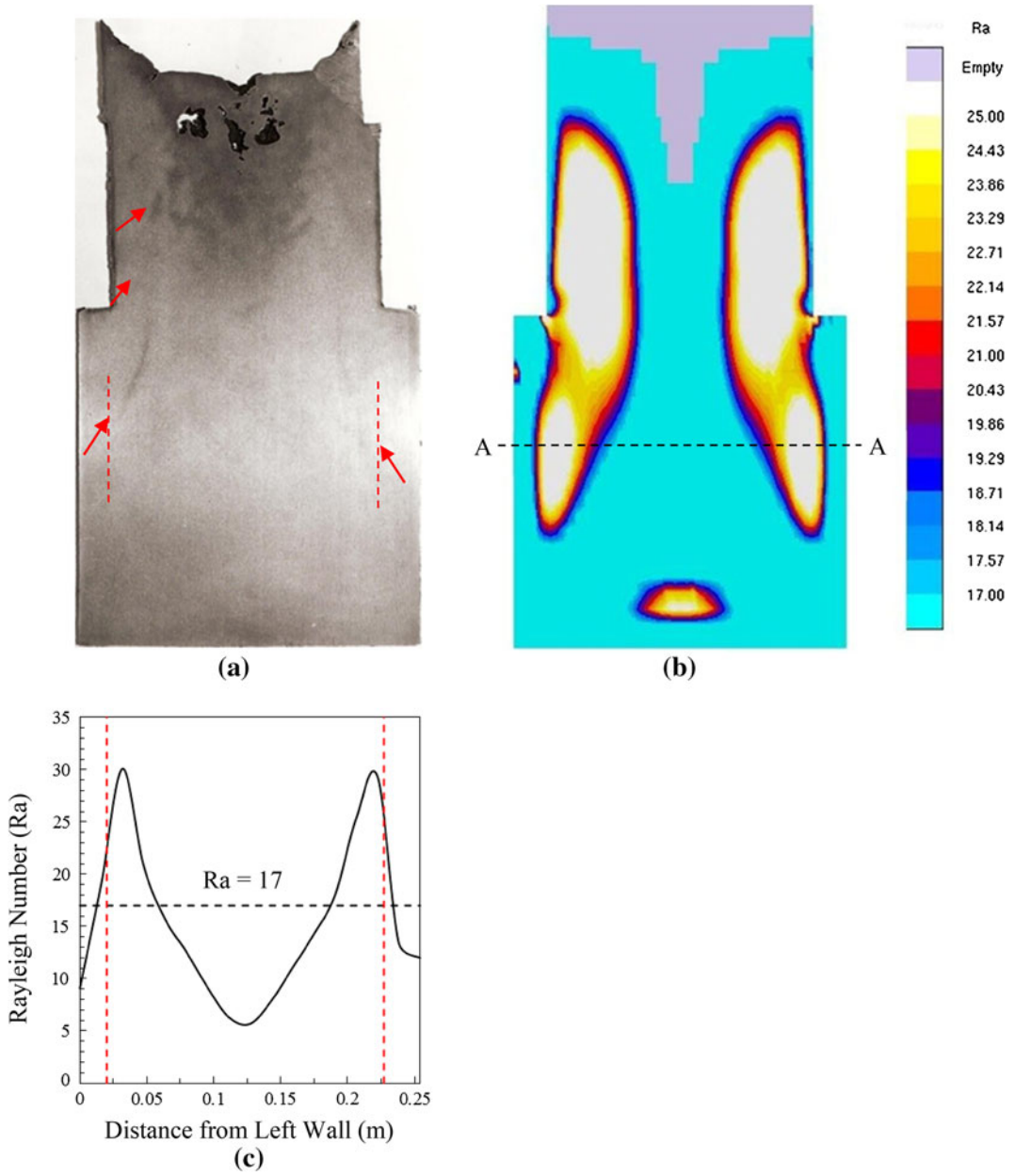

Fig. 6—Comparison of A-segregates (red arrows) observed in the cube casting with no breaker core and an exothermic hot topping: (*a*) with the predicted Rayleigh numbers, (*b*) for a vertical mid-thickness section. The predicted Rayleigh numbers along the dashed line A-A in (b) are plotted in (*c*). The vertical dashed lines in (a) and (c) indicate the onset of the A-segregates near the side walls. Photograph courtesy of Murphy.[41]

supercritical region that is predicted for all four cubes in the center near the bottom of the castings. There can be multiple reasons for this discrepancy. One possibility is that the center bottom portion of the cubes has an equiaxed grain structure, rather than a columnar one. A-segregates do not form in central equiaxed zones of castings. Another reason could be that at the bottom of the castings, the supercritical zone is not of sufficient height to support the melt convection patterns that are needed to sustain A-segregates. This was already noted by Schneider *et al.*[25] in their study of freckle formation in Ni-based superalloy castings. Therefore, the Rayleigh number criterion is more suitable for predicting regions in a casting where A-segregates do not form, rather than where they do form.

C. *Case Study 2-Forging Ram*

The second case study involves the steel forging ram casting shown in Figure 9. This case study is adopted from Kotas and Hattel,[43] where all details of the simulation settings are provided. The forging ram

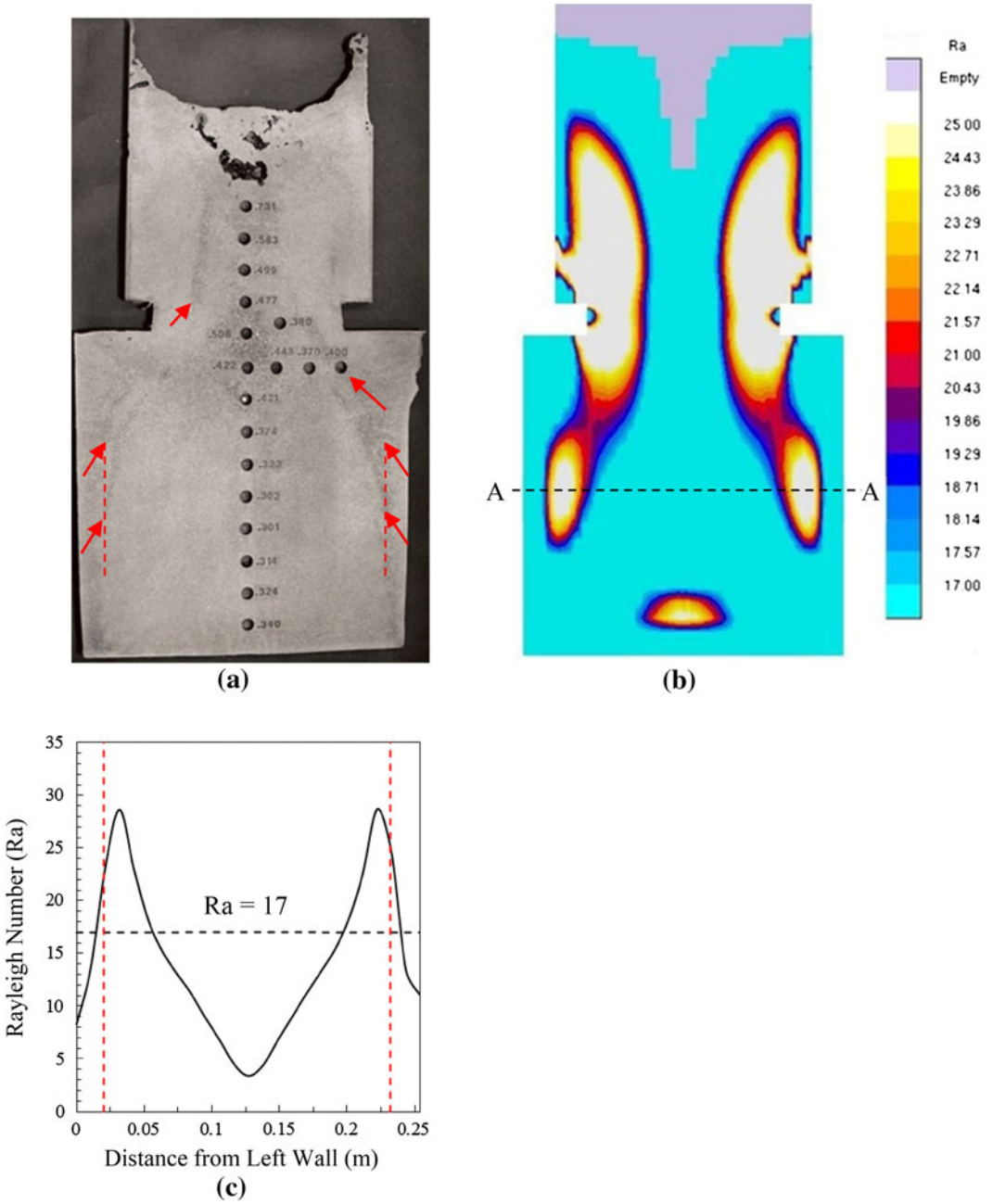

Fig. 7—Comparison of A-segregates (red arrows) observed in the cube casting with a 75 pct breaker core: (*a*) with the predicted Rayleigh numbers, (*b*) for a vertical mid-thickness section. The predicted Rayleigh numbers along the dashed line A-A in (b) are plotted in (*c*). The vertical dashed lines in (a) and (c) indicate the onset of the A-segregates near the side walls. Photograph courtesy of Murphy[41] (the numbers and holes should be ignored).

casting is more than 5.3 m (209 in.) tall and up to 2.3 m (91 in.) in diameter. The lower portion of the outer wall of the forging ram is chilled. The casting is fed using a single top riser with a sleeve.

Figure 10(a) shows that there are numerous A-segregates emanating near the vertical sidewalls in the bottom portion of the forging ram casting (red arrows). These A-segregates continue almost vertically along the sidewalls toward the upper portion of the casting (not shown). In addition, the center portion of the casting contains several V-segregates and porosity. The predicted Rayleigh number contours are shown in Figure 10(b). There are large regions parallel to the vertical sidewalls where the Rayleigh number is predicted to be greater than the critical value. These regions correspond reasonably well with the areas in the casting where A-segregates are observed. Figure 10(c) shows that, as in the cube castings, there are large gradients in the predicted Rayleigh number adjacent to the vertical sidewalls. Within the uncertainty of locating their origin

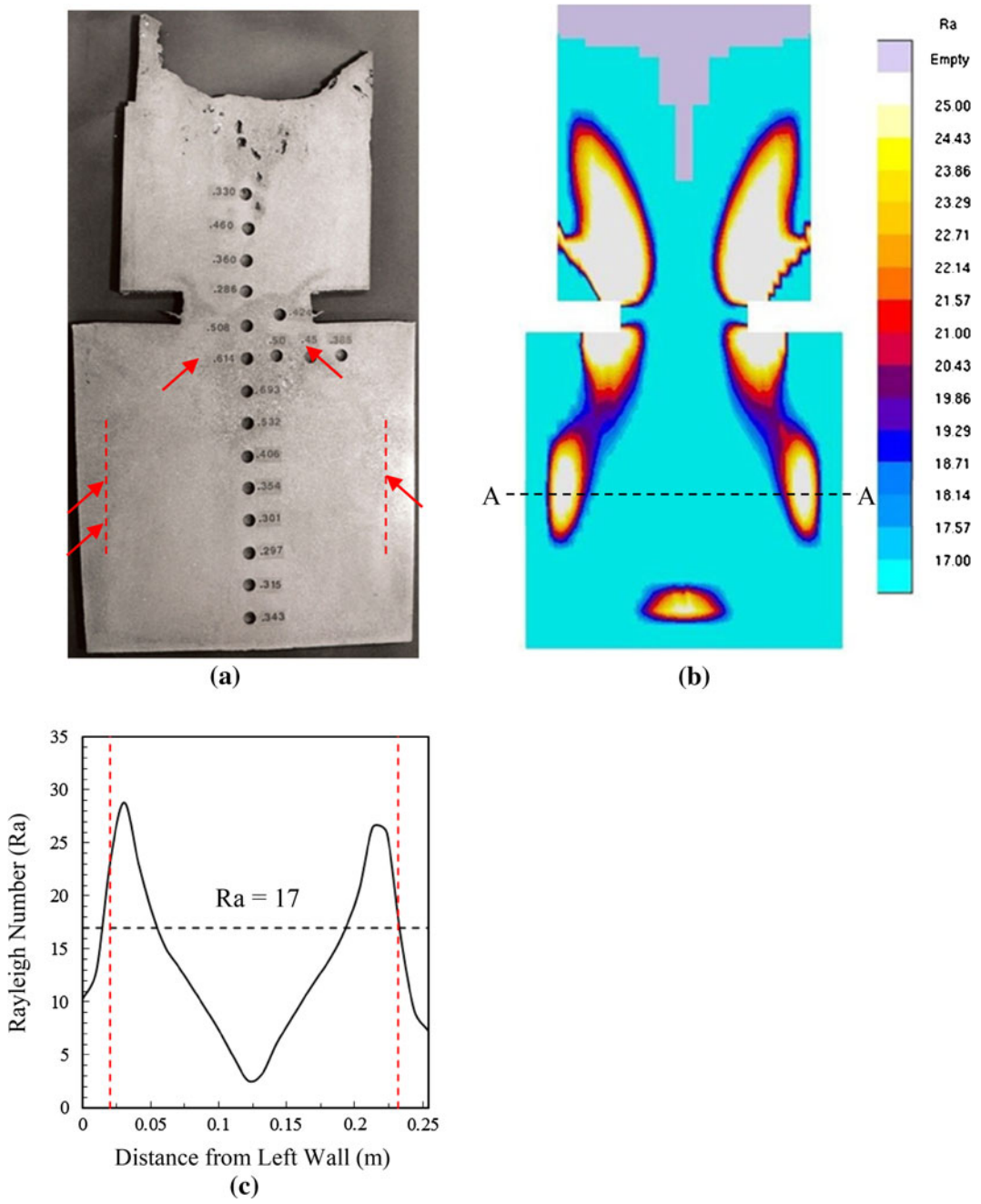

Fig. 8—Comparison of A-segregates (red arrows) observed in the cube casting with a 50 pct breaker core: (*a*) with the predicted Rayleigh numbers (*b*) for a vertical mid-thickness section. The predicted Rayleigh numbers along the dashed line A-A in (b) are plotted in (*c*). The vertical dashed lines in (a) and (c) indicate the onset of the A-segregates near the side walls. Photograph courtesy of Murphy[41] (the numbers and holes should be ignored).

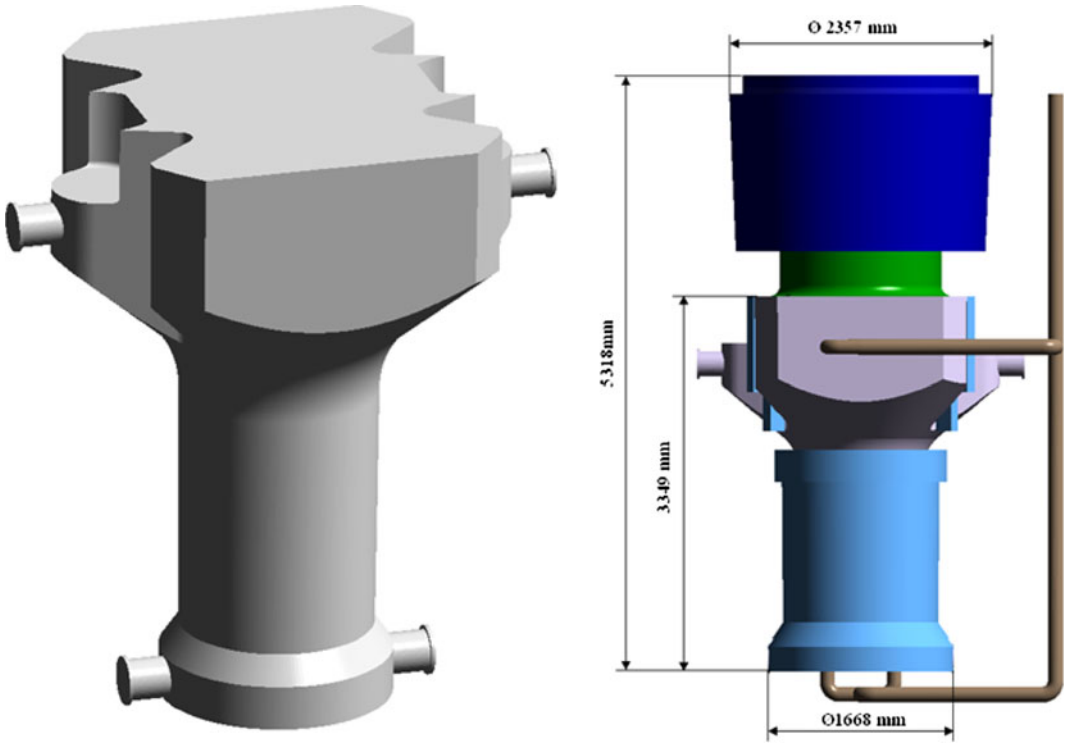

Fig. 9—Three-dimensional computer drawings of the forging ram casting of case study 2. Left panel: geometry of the machined forging ram; right panel: casting with rigging (light purple: casting; light blue: chills; green: riser; dark blue: riser sleeve; brown: gating system).

on the casting section (Figure 10(a)), the onset of the A-segregates can be seen to correspond well to a critical Rayleigh number of 17 ± 8.

The supercritical regions next to the sidewalls extend much further to the bottom and center of the casting than the areas where A-segregates are observed (see Figure 10(a)). There is also an isolated large region with super-critical Rayleigh numbers predicted at the very bottom of the casting. Again, no A-segregates are present there. These discrepancies can be directly attributed to the fact that the central and bottom portions of the casting have an equiaxed grain structure. The grain structure in the bottom portion of the forging ram casting is shown in Figure 10(d). As mentioned in the previous section, A-segregates do not form in central equiaxed zones of castings. Hence, if the Rayleigh number criterion of the current study could be combined with a simulation of the columnar-to-equiaxed transition, then the prediction of A-segregates could be improved.

Kotas and Hattel[43] applied the original Suzuki criterion to predict the A-segregates observed in the forging ram casting of the current study. By performing simulations with different critical Suzuki numbers, and comparing the results with the observations in Figure 10(a), they found that the value of the critical Suzuki number for the forging ram casting is 0.4 K min^{-1}(mm min^{-1})$^{1.1}$. Using Eqs. [1] and [14], together with a critical Rayleigh number of 17, $R = 28\ \mu m\ s^{-1}$ (as discussed in Section III–B), and the carbon content and density inversion from Table III, the same value of the critical Suzuki number is obtained here.

D. *Case Study 3-Ring*

In the third case study, A-segregates are investigated for the large steel rings and casting shown in Figure 11. The outer diameter of the ring is 7.74 m (305 in.). The height (excluding the riser) and width of the wall of the ring are 0.85 m (33 in.) and 0.64 m (25 in.), respectively. Both the outer and inner vertical surfaces of the ring are chilled. The riser extends over the entire top surface of the ring. On the vertical section through the wall of the machined ring in Figure 12(a), numerous A-segregates can be observed along both the outer and the inner vertical surfaces. Note that the machining of the inner surface of the ring wall results in the A-segregates extending almost all the way to the surface. At the inner surface, A-segregates are present over almost the entire height of the ring wall, whereas at the outer surface A-segregates are formed only in the upper portion.

The predicted Rayleigh number contours are shown in Figure 12(b). Overall, the regions containing A-segregates are predicted well. In particular, the fact that no A-segregates are observed in the lower portion of the ring wall near the outer surface is also reflected by the Rayleigh number contours. The absence of A-segregates in this region of the casting can therefore be explained by the higher cooling rates there. Figure 12(c) shows that, again, there are large gradients in the predicted Rayleigh number adjacent to the inner and outer surfaces. Within the uncertainty of locating their origin on the casting section (Figure 12(a)), the onset of the A-segregates can be seen to correspond well to a critical Rayleigh number of 17 ± 8. As in the previous two case

studies, the region where the Rayleigh number is predicted to be greater than the critical value extends too far to the central and the bottom of the wall. No A-segregates form in the center and bottom portions of the ring wall because the grain structure in these regions is presumably equiaxed.

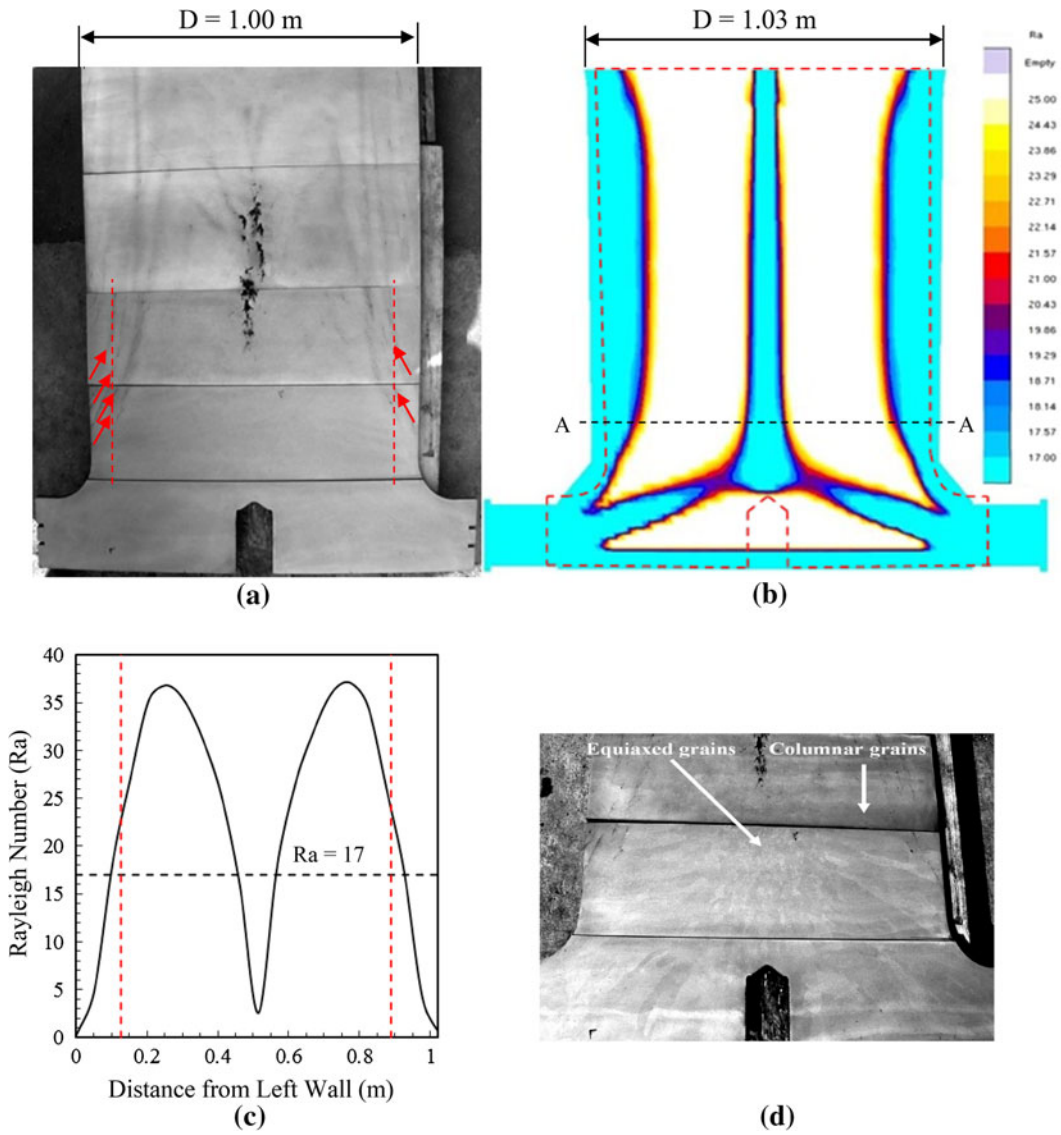

Fig. 10—Comparison of A-segregates (red arrows) observed in the lower portion of the machined forging ram (*a*) with the predicted Rayleigh numbers in the casting (*b*) for a vertical mid-thickness section. The dashed red line in (b) indicates the outline of the machined forging ram. The predicted Rayleigh numbers along the dashed line A-A in (b) are plotted in (*c*). The vertical dashed lines in (a) and (c) indicate the onset of the A-segregates near the side walls. The grain structure in the lower part of the casting is shown in (c). Photographs courtesy of Vitkovice Heavy Machinery a.s.

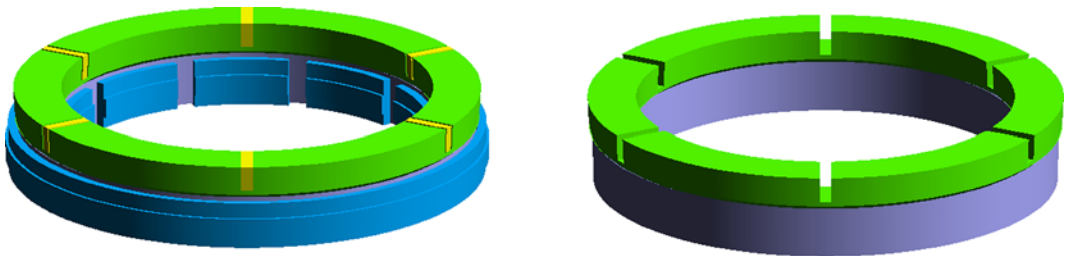

Fig. 11—Three-dimensional computer drawings of the steel ring casting of case study 3. Left panel: with chills and cores; right panel: casting with riser only (light purple: casting; light blue: chills; green: riser; yellow: core). The outer diameter of the ring is 7.74 m (305 in.).

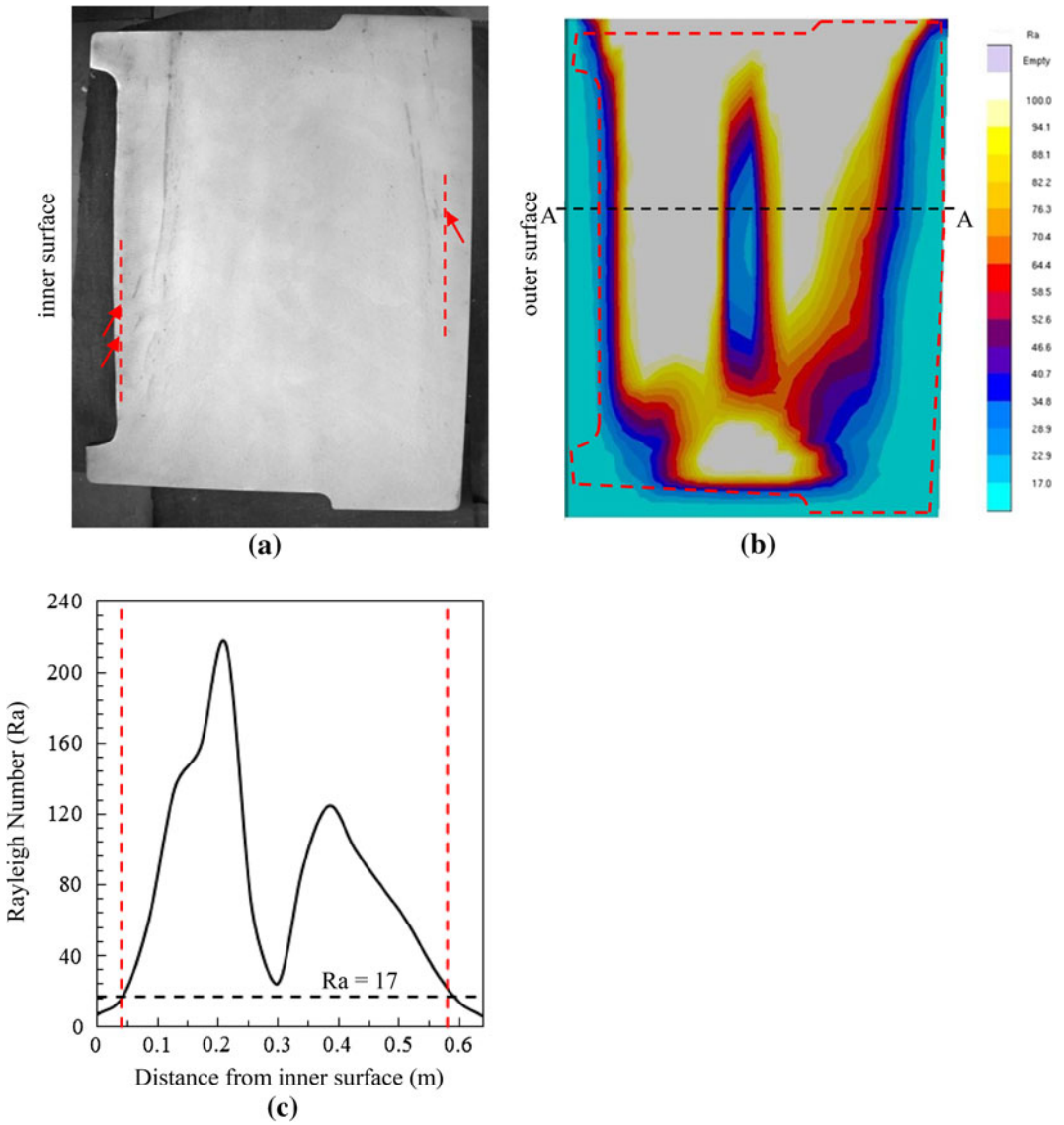

Fig. 12—Comparison of A-segregates (dashed red rectangles) observed in the wall of the machined steel ring (*a*) with the predicted Rayleigh numbers in the casting (*b*). The dashed black line in (b) indicates the outline of the machined steel ring wall. The predicted Rayleigh numbers along the dashed line A-A in (b) are plotted in (*c*). The vertical dashed lines in (a) and (c) indicate the onset of the A-segregates near the vertical surfaces of the ring. Photograph courtesy of Vitkovice Heavy Machinery a.s.

V. CONCLUSIONS

A Rayleigh number-based criterion is developed for predicting the formation of A-segregates in steel castings and ingots. The Rayleigh number is a function of the thermal gradient, cooling rate, liquid density inversion, and primary dendrite arm spacing over the first 30 pct of the semi-solid mush forming during solidification. Using experimental data from previous studies,[4,5] the critical value of the Rayleigh number is found to be 17 ± 8. At lesser values, no A-segregates are expected to form. Within its uncertainty, the critical Rayleigh number is the same for any steel composition. It is shown that the Rayleigh number is quite sensitive to the relation used for evaluating the dendrite arm spacing. Available dendrite arm spacing relations for steel do not always take into account the primary solidification mode (ferrite or austenite) and the effect of the various alloying elements present in the steel. In lieu of a better relation, the use of the one by Won and Thomas[39] is recommended.

Three case studies are presented where the Rayleigh number criterion of the current study is applied to predict A-segregates in shaped steel sand castings. The local thermal parameters are obtained from a standard casting simulation. By comparing the predictions with observations made in the actual castings, the Rayleigh number criterion is shown to correctly predict the regions where no A-segregates form. The spread in the value of the critical Rayleigh number (17 ± 8) of the current study corresponds approximately to the uncertainty in finding the exact location of the onset of the A-segregates on the casting sections. The regions where A-segregates form are somewhat overpredicted. Based

on the results of the three case studies, the primary reason for this overprediction is believed to be the presence of a central zone of equiaxed grains in the casting sections. A-segregates only form in the outer columnar zone and not when the grain structure is equiaxed.

REFERENCES

1. J.J. Moore and N.A. Shah: *Int. Mat. Rev.*, 1983, vol. 28, pp. 338–56.
2. S.M. Copley, A.F. Giamei, S.M. Johnson, and M.F. Hornbecker: *Metall. Trans.*, 1970, vol. 1, pp. 2193–2204.
3. T.M. Pollock and W.H. Murphy: *Metall. Mater. Trans. A*, 1996, vol. 27A, pp. 1081–94.
4. K. Suzuki and T. Miyamoto: *Trans. Iron Steel Inst. Jpn*, 1978, vol. 18, pp. 80–89.
5. H. Yamada, T. Sakurai, and T. Takenouchi: *J. Iron Steel Inst. Jpn.*, 1989, vol. 75, pp. 97–104.
6. P. Nandapurkar, D.R. Poirier, J.C. Heinrich, and S. Felicelli: *Metall. Trans. B*, 1989, vol. 20B, pp. 711–21.
7. J.C. Heinrich, S. Felicelli, P. Nandapurkar, and D.R. Poirier: *Metall. Trans. B*, 1989, vol. 20B, pp. 883–91.
8. M.G. Worster: *J. Fluid Mech.*, 1992, vol. 237, pp. 649–69.
9. G. Amberg and G.M. Homsy: *J. Fluid Mech.*, 1993, vol. 252, pp. 79–98.
10. D.M. Anderson and M.G. Worster: *J. Fluid Mech.*, 1995, vol. 252, pp. 307–31.
11. M.G. Worster: *Annu. Rev. Fluid Mech.*, 1997, vol. 29, pp. 91–122.
12. J.R. Sarazin and A. Hellawell: *Metall. Trans. A*, 1988, vol. 19A, pp. 1861–71.
13. S. Tait and C. Jaupart: *J. Geophys. Res.*, 1992, vol. 97, pp. 6735–56.
14. M.I. Bergman, D.R. Fearn, J. Bloxham, and M.C. Shannon: *Metall. Mater. Trans. A*, 1997, vol. 28A, pp. 859–66.
15. C. Beckermann, J.P. Gu, and W.J. Boettinger: *Metall. Mater. Trans. A*, 2000, vol. 31A, pp. 2545–57.
16. W. Yang, W. Chen, K. Chang, S. Mannan, and J. deBarbadilli: *Metall. Mater. Trans. A*, 2001, vol. 32A, pp. 397–405.
17. J.C. Ramirez and C. Beckermann: *Metall. Mater. Trans. A*, 2003, vol. 34A, pp. 1525–36.
18. S.N. Tewari and R. Tiwari: *Metall. Mater. Trans. A*, 2003, vol. 34A, pp. 2365–76.
19. L. Yuan and P.D. Lee: *Acta Mater.*, 2012, vol. 60, pp. 4917–26.
20. M.C. Schneider and C. Beckermann: *Metall. Mater. Trans. A*, 1995, vol. 26A, pp. 2373–88.
21. C. Beckermann: *Int. Mater. Rev.*, 2002, vol. 47, pp. 243–61.
22. J. Guo and C. Beckermann: *Numer. Heat Transf. A Appl.*, 2003, vol. 44, pp. 559–76.
23. K.D. Carlson and C. Beckermann: *Int. J. Cast Met. Res.*, 2012, vol. 25, pp. 75–92.
24. J.A. Dantzig and M. Rappaz: *Solidification*, 1st ed., EPFL Press, Lausanne, 2009, pp. 127–32.
25. M.C. Schneider, J.P. Gu, C. Beckermann, W.J. Boettinger, and U.R. Kattner: *Metall. Mater. Trans. A*, 1997, vol. 28A, pp. 1517–31.
26. C. Cicutti and R. Boeri: *Scripta Mater.*, 2001, vol. 45, pp. 1455–60.
27. M. Imagumbai: *ISIJ Int.*, 1994, vol. 34 (11), pp. 896–905.
28. M. Imagumbai: *ISIJ Int.*, 1994, vol. 34 (12), pp. 986–91.
29. C.Y. Wang, S. Ahuja, C. Beckermann, and H.C. De Groh, III: *Metall. Mater. Trans. B*, 1995, vol. 26B, pp. 111–19.
30. N. Saunders, U.K.Z. Guo, X. Li, A.P. Miodownik, and J.Ph. Schille: *JOM*, 2003, vol. 55, pp. 60–65.
31. M. El-Bealy and B.G. Thomas: *Metall. Mater. Trans. B*, 1996, vol. 27B, pp. 689–93.
32. M.A. Taha, H. Jacobi, M. Imagumbai, and K. Schwerdtfeger: *Metall. Trans. A*, 1982, vol. 13A, pp. 2182–2241.
33. H. Jacobi and K. Schwerdtfeger: *Metall. Trans. A*, 1976, vol. 7A, pp. 811–20.
34. M.C. Flemings, D.R. Poirier, R.V. Barone, and H.D. Brody: *J. Iron Steel Inst.*, 1970, vol. 208, pp. 371–81.
35. G. Wei and Z. Miao-Young: *J. Iron Steel Res. Int.*, 2009, vol. 16, pp. 17–21.
36. A. Suzuki and Y. Nagaoka: *J. Jpn. Inst. Met.*, 1969, vol. 33, pp. 658–63.
37. M. Wolf: PhD Thesis, EPFL, Lausanne, 1978.
38. J. Miettinen, S. Louhenkilpi, H. Kytönen, and J. Laine: *Math. Comput. Simul.*, 2010, vol. 80, pp. 1536–50.
39. Y.M. Won and B.G. Thomas: *Metall. Mater. Trans. A*, 2000, vol. 32A, pp. 1755–67.
40. MAGMASOFT® v4.6, Magma GmbH, Aachen, Germany.
41. W.T. Adams, Jr. and K.W. Murphy: *AFS Trans.*, 1980, vol. 88, pp. 389–404.
42. K.D. Carlson and C. Beckermann: *64th Steel Founders Society of America Technical and Operating Conference, Paper No. 3.2*, Chicago, IL, 2010.
43. P. Kotas and J.H. Hattel: *Mater. Sci. Technol.*, 2012, vol. 28, pp. 872–78.